Ligand Binding and Inhibition of an Oxygen-Sensitive Soluble Guanylate Cyclase, Gyc-88E, from *Drosophila*†

Shirley H. Huang,§ Donald C. Rio,§,⊥ and Michael A. Marletta*,‡,§,||,⊥

Department of Molecular and Cell Biology and of Chemistry, California Institute for Quantitative Biosciences, and Division of Physical Biosciences, Lawrence Berkeley National Laboratory, University of California, Berkeley, California 94720-3220

Received August 30, 2007; Revised Manuscript Received October 17, 2007

ABSTRACT: Soluble guanylate cyclase (sGC) uses a ferrous heme cofactor as a receptor for NO and once bound activates the enzyme for the conversion of GTP to cGMP. The heme cofactor in sGC does not bind oxygen, thereby allowing it to selectively bind NO despite a cellular concentration of oxygen (μM) that is much higher than signaling concentrations of nitric oxide (nM). The molecular details of this ligand discrimination against oxygen have emerged and allowed for predictions regarding ligand specificity in the sGC family. The results reported here show that Gyc-88E from *Drosophila* is a hemoprotein that binds oxygen, as well as NO and CO. All three ligands form 6-coordinate complexes. Gyc-88E is active as a homodimer (5600 ± 243 nmol min^{-1} mg^{-1}) and is inhibited by O_2, CO, and NO (3.2-, 2.9-, and 2-fold, respectively). The K_m for GTP was 0.66 ± 0.15 mM in air (273 μM oxygen) and 0.82 ± 0.15 mM under anaerobic conditions. The K_i for oxygen was calculated to be 51 ± 28 μM. The biochemical properties of Gyc-88E are unique for guanylate cyclases and suggest a possible function as an oxygen sensor.

Nitric oxide is a signaling molecule essential for vasodilation, short-term memory, and platelet aggregation. The enzyme soluble guanylate cyclase (sGC)[1] is a receptor for NO and once activated converts GTP to cGMP (*3*). A distinguishing feature of sGC is that it shows no measurable affinity for oxygen despite the presence of a ferrous protoporphyrin IX prosthetic group ligated to a histidine residue, identical to that in the globins. The heme cofactor is the binding site for NO. The lack of O_2 binding allows sGC to function as a selective NO sensor even in the presence of a much higher concentration of O_2 (*3*). Homologues of the sGC heme domain have recently been identified via phylogenetic approaches and form the H−NOX (heme−nitric oxide- and/or −oxygen-binding) family of proteins (*4*). Interestingly, some H−NOXs from obligate anaerobes bind O_2 with high affinity (nM), suggesting a role as oxygen sensors (*5*). The structure of an O_2-binding H−NOX from *Thermoanaerobacter tengcongensis* pointed toward the importance of a distal pocket tyrosine in the ability to bind O_2, and mutagenesis experiments have supported the critical importance of this residue (*5*−*8*). In fact, homology models derived from the *T. tengcongensis* H−NOX structure showed this distal pocket tyrosine to be absent in all H−NOXs that do not bind O_2 and to be present in those that are competent to bind O_2 (*4*, *9*).

Results with some of the predicted sGCs in *Caenorhabditis elegans* and *Drosophila melanogaster* suggest the ability to bind O_2 (*6*, *10*−*12*). Multiple sequence alignments (Figure 1A) with the O_2-binding *Tt*-H−NOX structure (*8*) indicate this tyrosine is present in the *Drosophila* atypical sGCs, thus predicting O_2 to be a potential ligand. In *C. elegans*, aerotaxis studies with knockouts have shown GCY-35, a predicted sGC, to be essential for avoidance of high O_2 levels (*10*). Although the purified heme domain of GCY-35(1−252) does bind O_2 (*10*), there has been no direct demonstration from purified GCY-35 that it has guanylate cyclase activity that could be regulated by O_2. Since these observations, a wealth of biochemical results and homology models have provided the basis for prediction of ligand-binding properties, specifically the ability to discriminate against O_2 binding in a subset of H−NOX proteins.

In *D. melanogaster*, there are five genes encoding soluble guanylate cyclases that all contain a predicted H−NOX domain, a PAS-like domain, a coiled-coil region, and a catalytic domain (*13*, *14*). Two of these genes, *Dm*GC-α1 and *Dm*GC-*β*1,[2] encode typical NO-regulated sGCs (*1*, *2*, *15*) that are predicted to not bind O_2. These sGCs are expressed predominantly in adult fly heads and, while not extensively characterized, have been linked to cGMP-

† This work was supported, in part, by a National Science Foundation Predoctoral Fellowship to S.H.H. and National Institutes of Health Research Grants GM070671 to M.A.M. and GM48862 to D.C.R.

* To whom correspondence should be addressed. Phone: (510) 666-2763. Fax: (510) 666-2765. E-mail: marletta@berkeley.edu.

‡ Department of Chemistry.

§ Department of Molecular and Cell Biology.

|| Division of Physical Biosciences, Lawrence Berkeley National Laboratory.

⊥ California Institute of Quantitative Biosciences.

[1] Abbreviations: sGC, soluble guanylate cyclase; NO, nitric oxide; GTP, guanosine triphosphate; cGMP, cyclic 3′,5′-guanosine monophosphate; H−NOX, heme−nitric oxide- and/or −oxygen-binding domain; PAS, Per/Arnt/Sim protein family; PKG, cGMP-dependent protein kinase; COS-7, African green monkey kidney cell; FBS, fetal bovine serum; DEA-NO, diethylammonium (*Z*)-1-(*N*,*N*-diethylamino)-diazen-1-ium-1,2-diolate; DTT, dithiothreitol; HEPES, 4-(2-hydroxyethyl)-1-piperazineethanesulfonic acid; K_i, dissociation constant for the enzyme/inhibitor complex.

[2] *Dm*GC-α1 and *Dm*GC-*β*1 have previously been referred to as Dgcα1 (*1*) and Dgc*β*1 (*1*, *2*), respectively.

10.1021/bi701771r CCC: $37.00
Published on Web 11/29/2007

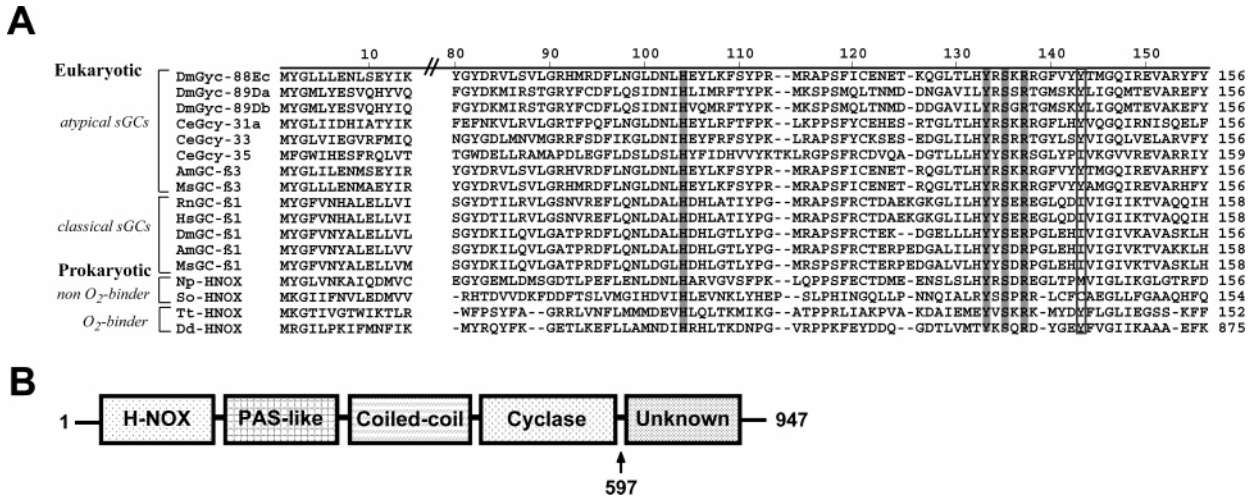

FIGURE 1: Multiple sequence alignment of several H−NOX proteins and the domain architecture of Gyc-88E. (A) Multiple sequence alignment of the heme domain of various H−NOXs, which include eukaryotic sGCs and bacterial H−NOX proteins. The numbering corresponds to the Gyc-88Ec sequence. The specific residues that are predicted to be important for heme (highlighted) and oxygen binding (boxed) are discussed in the text. Alignments were generated using the Clustal W algorithm (*37*) in MegAlign. Accession numbers for all protein sequences are listed in the Materials and Methods. (B) Predicted domain architecture of full-length Gyc-88E. Gyc-88E has the same predicted domains as known sGCs (*13*), but also contains an extra domain of unknown function at the C-terminus. Gyc-88E(1−597) consists of all domains except for the C-terminal domain.

dependent protein kinase (PKG) activity and foraging behaviors (*1*, *2*, *16*). The three other genes, Gyc-89Da, Gyc-89Db, and Gyc-88E, encode atypical sGCs that we predict could bind O_2 and, therefore, might be regulated by O_2. Homology models of these proteins with the *T. tengcongensis* H−NOX show a distal pocket tyrosine within hydrogen-bonding distance to an iron-bound O_2. Others have suggested that these atypical sGCs are potentially regulated by O_2 (*15*). Gyc-88E is 34% identical to rat sGC β1 and 31−33% identical to Gyc-89Da and Gyc-89Db. These atypical sGCs are expressed during embryonic, larval, and adult life stages in various neurons in the head and in peripheral nervous system neurons that innervate the trachea and chemosensory organs (*15*). On the basis of multiple sequence alignments of the catalytic domains of various guanylate cyclases and homology models with adenylate cyclase (*11*, *17*), Gyc-88E contains all residues crucial for activity normally contributed by both sGC α1 and β1 subunits and therefore is predicted to be active as a homodimer. Gyc-89Da and Gyc-89Db, which are missing a crucial aspartate residue normally contributed by sGC α1, are predicted to be inactive as homodimers but active as a heterodimer with Gyc-88E (*11*). These predictions are consistent with lysate assays from COS-7 cells expressing various combinations of the fly atypical sGCs (*18*). However, there has been no report of O_2 binding or guanylate cyclase activity from a purified atypical sGC to establish conclusively that any of these homologues are indeed sGCs that can be regulated by O_2. In this study, we have successfully purified a *Drosophila* atypical sGC, Gyc-88E. Electronic absorption spectra were acquired for various gaseous ligand complexes, and the effect of each ligand on cyclase activity was measured. Distinct from NO-regulated sGC, Gyc-88E binds and is inhibited by O_2, as well as NO and CO.

MATERIALS AND METHODS

Materials. CO gas (>99% pure) was purchased from Praxair, Inc., and diethylammonium (*Z*)-1-(*N*,*N*-diethylamino)-diazen-1-ium-1,2-diolate (DEA-NO) was purchased from Cayman Chemical Co. cGMP enzyme immunoassay kits, format B, were obtained from Biomol. Reacti-Vials were purchased from Pierce. Primers were purchased from Elim Biopharmaceuticals. Restriction enzymes were obtained from New England Biolabs, and DNA polymerases were from Roche. All protease inhibitors, except for Pefabloc SC (Centerchem, Inc.), were from Research Products International Corp. All other chemicals were from Sigma unless otherwise stated.

Cloning. DNA of Gyc-88E (clone SD08665), which contains all introns but lacks the last 492 base pairs, was obtained from the Drosophila Genomics Resource Center. The last 492 base pairs of Gyc-88E were PCR-amplified from a *D. melanogaster* embryonic cDNA library (gift from Dr. Svetlana Dzitoyeva, University of Illinois) using the forward primer 5′-CAATTCCACGGGCCACGTGTTTATGCGAAC-3′ and the reverse primer 5′-CCTGGCTGGTGCCGAGTTAGATCGATG-3′. A 3′-*Sal*I restriction site was then introduced by PCR amplification using the same forward primer and the reverse primer 5′-CTTCTCGTCGACCCTGGCTGGTGCCGAGTTAGATCGATG-3′. The 492 base pair product was inserted into SD08665-pOT2 at the *Pml*I and *Sal*I sites to generate the full-length intron-containing Gyc-88E DNA. This full-length Gyc-88E was then subcloned into the pMT/V5HisA *Drosophila* expression vector at the *Spe*I and *Age*I restriction sites. To obtain full-length, intronless Gyc-88E cDNA, mRNA was isolated by reverse transcription with oligo$(dT)_{14}$ primers from *Drosophila* Schneider 2 (S2) cells stably transfected with the Gyc-88E/pMTV5HisA intron-containing construct. PCR with the forward primer 5′-CGCCTCGAG-CAAAATGTACGGACTGCTGCTGGAGA-3′ (containing the consensus *Drosophila* Cavener sequence underlined) (*19*) and the reverse primer 5′-GCGTCTAGAGTTCTCTCGTTCCTCCAGCCAGT-3′ was then used to insert Gyc-88E(1−597) into the pUChygMTpy2 *Drosophila* expression vector at the *Xho*I and *Xba*I sites. All constructs

were confirmed by DNA sequencing (UC Berkeley DNA Core Facility).

Cell Culture and Transfection. A stable S2 cell line containing Gyc-88E(1−597)/pUChygMTpy2 was generated using standard calcium phosphate transfection (*20*) and selection in 200 μg/mL hygromycin. The presence of the Gyc-88E(1−597) protein containing a C-terminal tandem polyoma (EYMPMEEYMPME) tag was confirmed by Western blot analysis using a mouse monoclonal anti-polyoma antibody (Covance). The cell line was maintained in Insect-XPress medium (Lonza) containing 5% FBS (Hyclone), 50 μg/mL hygromycin, and 1% antibiotic−antimycotic (Gibco) in 25 cm^2 T-flasks at 25 °C.

Expression. S2 cultures containing Gyc-88E(1−597) were expanded to 5 L in Insect-XPress medium with 5% FBS and 1% antibiotic−antimycotic in spinner flasks (Bellco Glass). At a cell density of 4×10^6/mL, expression was induced by 7 μM $CuSO_4$ at 25 °C. Two days after induction, the cells were harvested by centrifugation at 4000 rpm for 10 min at 4 °C, and the pellet was washed with phosphate-buffered saline and frozen at −80 °C.

Purification. All steps of the purification were carried out at 4 °C. Frozen pellets from 5 L of S2 cells were thawed on ice and resuspended in 100 mL of buffer A (25 mM HEPES, pH 7.4, 150 mM NaCl, 5% glycerol, 1 mM β-mercaptoethanol, 1 μM pepstatin A, 1 μM leupeptin, 0.17 μM aprotinin, 0.5 μg/mL E-64, and 2 mM Pefabloc SC). The cells were lysed by sonication (Misonix Sonicator 3000), and the lysate was centrifuged at 200000*g* for 1.5 h. A 0.4 mL anti-polyoma column composed of anti-polyoma IgG immobilized on Fast Flow Sepharose beads (Covance Research Products) was equilibrated with 2 mL of buffer A. The supernatant was applied to the anti-polyoma column at a flow rate of 0.4 mL/min. The column was washed with 2 mL of buffer A, followed by 2 mL of buffer B (25 mM HEPES, pH 7.4, 500 mM NaCl, 0.1 mM EDTA, 5% glycerol, 1 mM β-mercaptoethanol, 1 μM pepstatin A, and 1 μM leupeptin) and 1.2 mL of buffer A. Polyoma-tagged Gyc-88E(1−597) protein was eluted with 2.4 mL of 25 μg/mL EYMPME peptide (>95% purity, synthesized by Elim Pharmaceuticals) in buffer A, followed by 2.4 mL each of 50 μg/mL, 100 μg/mL, 500 μg/mL, and 1 mg/mL EYMPME. The presence of Gyc-88E(1−597) was determined by electronic absorption spectroscopy, and fractions containing an A_{278}/A_{415} ratio of ≤6 were pooled and concentrated to 0.2 mL in a Vivaspin-20 50K filter (Vivascience). The protein sample was then diluted into 7 mL of buffer C (25 mM triethanolamine, pH 7.5, 5 mM dithiothreitol) and loaded onto a prepacked POROS HQ2 anion-exchange column (Applied Biosystems) at 1 mL/min using a BioLogic Duo Flow (Bio-Rad Laboratories). The column was washed with 10 mL of buffer C at 2 mL/min, and a gradient from 0 to 750 mM NaCl in buffer C was applied over 50 mL at 1 mL/min. Fractions containing Gyc-88E(1−597) ($A_{278}/A_{415} \leq 1.2$) were collected and pooled. The protein was concentrated in a Vivaspin-6 10K filter and buffer exchanged into buffer D (50 mM HEPES, pH 7.4, 150 mM NaCl, 5% glycerol, 2 mM dithiothreitol). The concentrated protein was drop-frozen in liquid N_2 and stored at 77 K. Protein concentrations were determined by Bradford microassay (Bio-Rad Laboratories). Protein purity was assessed by SDS−PAGE with 10−20% Tris−glycine gels (Invitrogen) using Mark 12 unstained molecular weight markers (Invitrogen).

Analytical Gel Filtration. The native molecular weight of Gyc-88E(1−597) was determined on a Beckman HPLC system (126 NMP solvent module, 168 NM detector) equipped with a Zorbax GF-250 gel filtration column at 22 °C. The column was equilibrated in 200 mM potassium phosphate, pH 7.5, 150 mM NaCl buffer at 1 mL/min over 20 min. The sample injection volume was 20 μL. The standards used were cytochrome *c* (12.4 kDa), ovalbumin (45 kDa), bovine serum albumin (66 kDa), yeast alcohol dehydrogenase (150 kDa), and thyroglobulin (669 kDa). All standards were run in duplicate at 1 mg/mL, and Gyc-88E-(1−597) was at 1 mg/mL. Proteins were detected by absorbance at 278 nm, and heme was monitored at 415 nm. Standards were plotted as the log of molecular weight versus retention time, and data were fit to a line with a slope of −2.3973, a *y*-intercept of 14.521, and an R^2 of 0.9745.

Spectroscopic Characterization and Complex Formation. All spectra were recorded on a Cary 3E spectrophotometer equipped with a Neslab RTE temperature controller set at 22 °C in buffer D. The spectrum of the protein as purified was determined directly from a freshly thawed aliquot of Gyc-88E(1−597). The protein (0.7 μM) and buffer D were degassed and taken into an anaerobic chamber (Coy). To reduce the protein, $Na_2S_2O_4$ (62.5 mM in buffer D) was added to a final concentration of 0.5 mM and incubated at 4 °C for 5 min. Excess $Na_2S_2O_4$ was removed by buffer exchange using a Vivaspin-0.5 10K filter. The spectrum of the Fe(II)-unligated protein after buffer exchange (0.3 μM) was determined in an anaerobic quartz cuvette sealed with a rubber septum. To form the Fe(II)−CO protein, a sealed cuvette containing the reduced protein was exposed to 1 atm of CO gas for 8 min on ice (1 mM CO dissolved in water at 22 °C) (*21*). The spectrum of the Fe(II)−CO complex was acquired, and the protein was assayed in the anaerobic chamber. An aliquot of the Fe(II)-unligated protein was exposed to 1 atm of air (273 μM O_2 dissolved in water at 22 °C) (*21*) for 5 min at 22 °C to form the Fe(II)−O_2 complex. After the spectrum was acquired, the protein was assayed. A DEA-NO stock solution (500 μM DEA-NO in water) was added to a cuvette containing the Fe(II)−O_2 protein to achieve a final concentration of 10 μM DEA-NO. After 5 min at 22 °C, a spectrum of the resulting Fe(II)−NO protein was taken, and the complex was assayed. The protein concentrations were determined by Bradford microassay.

Activity Assays. Triplicate end-point assays were performed at 22 °C in 50 mM HEPES, pH 7.5, 30 mM NaCl, 1.5 mM GTP, 2 mM DTT, and 5 mM $MgCl_2$. The assay buffer used for the Fe(II)−CO and Fe(II)−NO complexes also contained 1 atm of CO gas and 10 μM DEA-NO, respectively. After confirmation of complex formation as described above, the enzyme was added to initiate the reaction. Final assay volumes were 100 μL and contained 0.01 μg of Fe(II)-unligated, Fe(II)−CO, and Fe(II)−O_2 protein and 0.05 μg of Fe(II)−NO protein. Electronic absorption spectroscopy was used to verify that all complexes were stable throughout the course of the assay. After 5 min, 400 μL of 125 mM $Zn(OAc)_2$ and 500 μL of 125 mM Na_2CO_3 were added to quench the reactions, which were frozen at −80 °C overnight. cGMP was quantified using a cGMP

enzyme immunoassay kit, Format B (Biomol), per the manufacturer's instructions. Assays were repeated three times to ensure reproducibility.

K_i for O_2 Inhibition. Duplicate end-point assays were carried out at each O_2 concentration. Buffer containing 273 μM O_2 was made by sealing 50 mM HEPES, pH 7.5, 2 mM DTT in a silicone-sealed Reacti-Vial under 1 atm of air at 22 °C (*21*). Deoxygenated 50 mM HEPES, pH 7.5, 2 mM DTT buffer was made in the anaerobic chamber. Fe(II)-unligated protein was produced as described above. The O_2 concentrations were achieved by dilution of appropriate volumes of 273 μM O_2 buffer into deoxygenated buffer and Fe(II)-unligated protein in sealed Reacti-Vials using gastight syringes (Hamilton) in the anaerobic chamber. After a 7 min equilibration, reactions were started by adding GTP−Mg^{2+}. Final assay volumes were 150 μL and contained 0.02 μg of Fe(II)-unligated protein, 20 mM NaCl, 8 mM GTP, and 20 mM $MgCl_2$. After 7 min, the reactions were quenched, and cGMP was quantified as described above. Data were fit via nonlinear regression (Kaleidagraph 4.0, Synergy Software) to the equation for hyperbolic mixed-type inhibition (*22*):

$$V_{\max_i} = V_{\max}\frac{1+\frac{\beta[I]}{\alpha K_i}}{1+\frac{[I]}{\alpha K_i}}$$

$V_{\max_i}$ is the apparent $V_{\max}$ at a particular concentration of O_2, $V_{\max}$ is that of the uninhibited Fe(II)-unligated enzyme, β is the ratio of the $V_{\max}$ in the presence of air to the $V_{\max}$ in the absence of air, α is the ratio of the K_m for GTP−Mg^{2+} in the presence of air to the K_m for GTP−Mg^{2+} in the absence of air, and K_i is the equilibrium dissociation constant of O_2 for inhibiting the enzyme. K_m values were determined by incubating Gyc-88E(1−597) (1.8 nM) for 7 min at 22 °C in 50 mM HEPES, pH 7.5, 30 mM NaCl, and 2 mM DTT with varying concentrations of GTP−Mg^{2+} under either air or argon. Reactions were quenched, and cGMP was quantified as described above. Data were fit by nonlinear regression (Kaleidagraph 4.0) to a standard Michaelis−Menten equation: $V = (V_{\max}[\text{GTP}-Mg^{2+}])/(K_m + [\text{GTP}-Mg^{2+}])$ (*22*).

GenInfo Identifier Numbers. *Dm*Gyc-88Ec (gi62484297), *Dm*Gyc-89Da (gi116008023), *Dm*Gyc-89Db (gi24647456), *Ce*Gcy-31a (gi30526294), *Ce*Gcy-33 (gi71996441), *Ce*Gcy-35 (gi71990145), *Ms*GC-β3 (gi3511174), *Am*GC-β3 (gi60458816), *Rn*GC-β1 (gi52138592), *Hs*GC-β1 (gi4504214), *Dm*GC-β1 (gi24651576), *Am*GC-β1 (gi48596914), *Ms*GC-β1 (gi3372755), *Np*-H−NOX (gi23129606), *So*-H−NOX (gi24373702), *Tt*-H−NOX (gi20807169), *Dd*-H−NOX (gi23475919).

RESULTS

Spectral Characteristics of Gyc-88E. To examine the ligand-binding properties of Gyc-88E(1−597), this construct was expressed and purified to homogeneity. The first 597 residues of Gyc-88E contain predicted H−NOX, PAS-like, coiled-coil, and catalytic domains (Figure 1B). The 350 amino acid C-terminal domain of this protein is absent in sGC β1 proteins and is of unknown function, as a BLAST search against this domain identified no homologues. This domain could serve as an additional means of regulation, perhaps through interactions with other proteins, but further experiments are needed to elucidate its function.

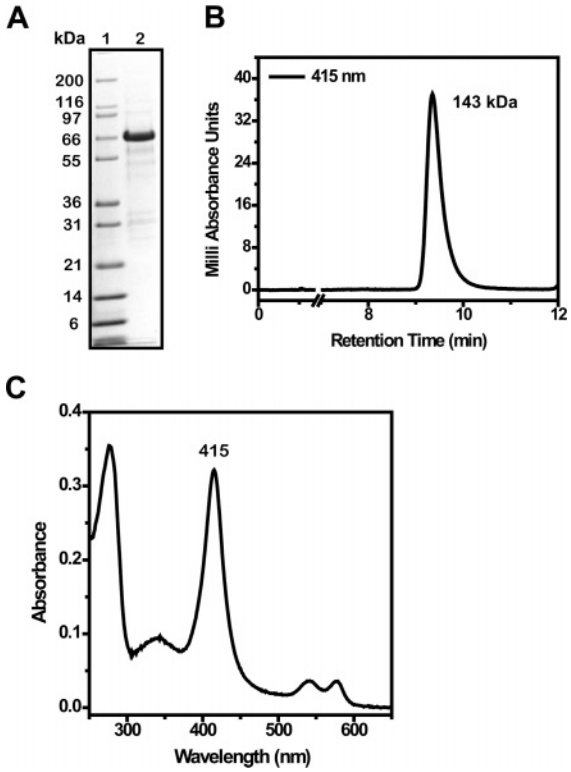

FIGURE 2: Gyc-88E(1−597) is a homodimer that purifies as an Fe(II)−O_2 complex. (A) SDS−PAGE analysis of Gyc-88E(1−597): lane 1, mark 12 molecular weight standards; lane 2, Gyc-88E(1−597) after purification (~7 μg). The protein sample appears to be >95% pure by gel with a molecular mass of ~68 kDa. (B) Analytical gel filtration of Gyc-88E(1−597). There is one main peak at 9.4 min, which absorbs at 415 nm. On the basis of this retention time, Gyc-88E(1−597) is a homodimer with a native molecular mass of 143 kDa. (C) UV−vis spectrum of Gyc-88E-(1−597) as purified (1.4 μM). The spectrum is characterized by a Soret absorbance maximum at 415 nm and split α/β bands at 542 and 577 nm. The approximate ratio of protein (278 nm) to heme (415 nm) absorbance is 1:1.

Gyc-88E(1−597) was cloned and expressed in S2 cells as a polyoma-tagged construct under the control of the metallothionein promoter. Gyc-88E expression was increased without the C-terminal domain, and Gyc-88E(1−597) has activity and spectroscopic characteristics similar to those of the full-length protein (data not shown). Due to increased protein expression, our study focused on the truncated atypical sGC. Gyc-88E(1−597) was purified to >95% purity, as shown by the single 68 kDa band on the denaturing gel (Figure 2A). Analytical gel filtration revealed that Gyc-88E-(1−597) is a homodimer with a native molecular mass of 143 kDa, close to the predicted mass of 136 kDa for a dimer (Figure 2B). The catalytic domains of this construct contain the residues shown to be required for catalytic activity in NO-sensitive sGC, and consequently, Gyc88E(1−597) was expected to be active as a homodimer (*11*, *17*). As the alignment and homology model predict, Gyc-88E(1−597) is isolated as an Fe(II)−O_2 complex, with a Soret absorbance maximum at 415 nm and split α/β bands at 542 and 577 nm (Figure 2C). The spectrum is characteristic of 6-coordinate, low-spin Fe(II)−O_2 complexes in both H−NOXs and globins (*9*, *23*). The Soret absorbance maximum shifts to 421 nm upon CO addition and remains at 415 nm after potassium

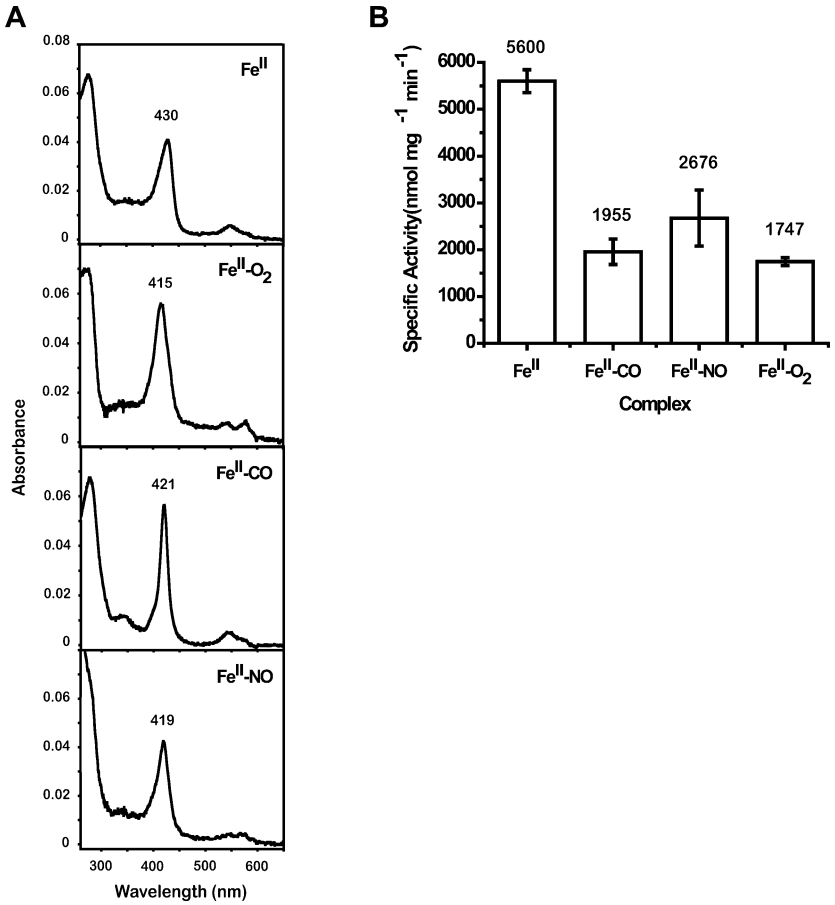

FIGURE 3: UV−vis spectrum and activities of Gyc-88E(1−597) complexed to various gaseous ligands. (A) UV−vis spectrum of Gyc-88E(1−597) complexed to O_2, NO, and CO. The Fe(II)-unligated protein has a Soret absorbance maximum at 430 nm. When bound to O_2, CO, or NO, the Soret absorbance maximum shifts to 415, 421, and 419 nm, respectively. The protein concentration was 278 nM. (B) Activities of the Gyc-88E(1−597) ligand complexes. Activity assays with purified Gyc-88E(1−597) (0.01 μg of Fe(II), Fe(II)−O_2, and Fe(II)−CO and 0.05 μg of Fe(II)−NO) were performed in 50 mM HEPES, pH 7.5, 30 mM NaCl, 1.5 mM GTP, 2 mM DTT, and 5 mM $MgCl_2$. Ligand concentrations in the assay buffer were 273 μM O_2, 1 mM CO, and 10 μM DEA-NO. Gyc-88E(1−597) is inhibited by O_2, NO, and CO. This mechanism of regulation is highly distinct from that of classical sGCs, which are insensitive to oxygen and activated by NO and CO.

cyanide addition (data not shown), indicating a ferrous oxidation state as purified. The protein remains stable as an Fe(II)−O_2 complex throughout the course of the 2 day purification. The stability of the ferrous oxidation state is like that seen with the classical sGCs, suggesting that, like those, the ferric oxidation is not relevant under normal physiological conditions.

The formation of various heme complexes was investigated with purified Gyc-88E(1−597) by UV−vis spectroscopy. Gyc-88E(1−597) forms stable complexes with O_2, NO, and CO (Figure 3A). The spectrum of the Fe(II)−O_2 complex formed after reduction and exposure to air was identical to that of the as-purified protein. Upon addition of CO gas to the Fe(II)-unligated protein (278 nM), a characteristic 6-coordinate, low-spin Fe(II)−CO complex was formed with a Soret absorbance maximum at 421 nm and split α/β bands. This spectrum is similar to those of the Fe(II)−CO complexes of other characterized H−NOXs (Table 1) (*6*, *10*, *24*, *25*). Upon addition of 10 μM DEA-NONOate to the Fe(II)−O_2 protein (278 nM), a characteristic 6-coordinate, low-spin Fe(II)−NO complex with a Soret absorbance maximum of 419 nm was formed within 5 min at 22 °C. In contrast, sGC β1 and multiple prokaryotic non-oxygen-binding H−NOXs bind NO as a 5-coordinate complex (Table 1) (*6*, *24*, *25*). All oxygen-binding H−NOXs characterized thus far, GCY-35(1−252) and *Tt*-H−NOX, bind NO to form a mostly 6-coordinate complex (*6*, *10*, *24*). The formation of a 6-coordinate Gyc-88E(1−597) Fe(II)−NO complex is consistent with this trend and may be due to a weakening of the NO trans effect by the distal pocket tyrosine (*24*). Overall, the ligand-binding properties are very much like those observed with the globins (*23*). Further spectroscopic studies are in progress to examine the heme environment of Gyc-88E and to confirm the ligation state of the complexes.

Table 1: UV−vis Peak Positions[a] for Various Fe(II) Protein Complexes

ligand	protein	Soret	β	α	ref
none	Gyc-88E(1−597)	430	555		this work
	Tt-H−NOX	431	565		*6*
	sGC (α1/β1)	431	555		*25*
O_2	Gyc-88E(1−597)	415	541	577	this work
	Tt-H−NOX	416	556	591	*6*
	sGC (α1/β1)	does not bind			*25*
NO	Gyc-88E(1−597)	419	544	572	this work
	Tt-H−NOX	420	547	575	*6*
	sGC (α1/β1)	398	537	572	*25*
CO	Gyc-88E(1−597)	421	543	570	this work
	Tt-H−NOX	424	544	565	*6*
	sGC (α1/β1)	423	541	567	*25*

[a] Nanometers (at 22 °C).

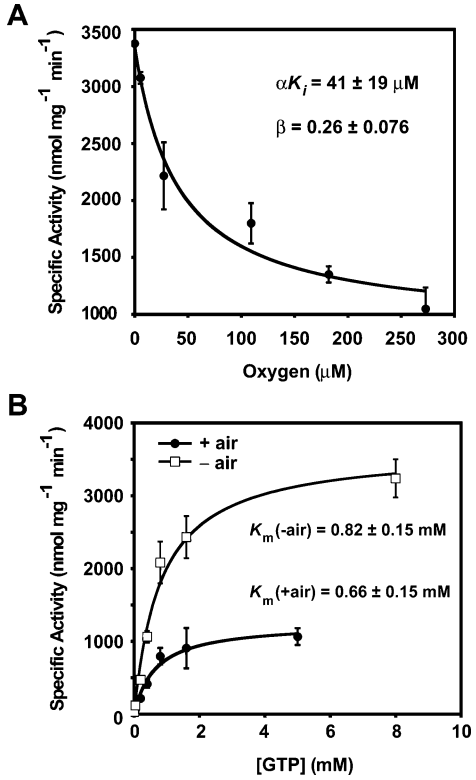

FIGURE 4: Determination of the affinity of Gyc-88E(1−597) for O_2 and the dependence of the K_m for GTP−Mg^{2+} on O_2. (A) Activity of Gyc-88E(1−597) with varying concentrations of O_2. Activity assays with purified Gyc-88E(1−597) (0.02 μg) were performed in 50 mM HEPES, pH 7.5, 2 mM DTT, 20 mM NaCl, 8 mM GTP, 20 mM $MgCl_2$, and varying O_2 concentrations. The K_i was calculated to be 51 ± 28 μM. (B) Determination of K_m in the presence and absence of air. Activity assays with purified Gyc-88E(1−597) (0.02 μg) were performed in oxygenated (273 μM O_2) and deoxygenated buffer (50 mM HEPES, pH 7.5, 2 mM DTT, 30 mM NaCl, and varying concentrations of GTP−Mg^{2+}). K_m values in the presence and absence of O_2 were 0.66 ± 0.15 and 0.82 ± 0.15 mM, respectively.

Enzymatic Activity. In addition to binding, the effect of O_2, NO, and CO on guanylate cyclase activity was examined by triplicate 5 min end-point assays at 22 °C. Fe(II)-unligated Gyc-88E(1−597) had a specific activity of 5600 ± 243 nmol min^{-1} mg^{-1} (Figure 3B), which is of the same order of magnitude as that of NO-stimulated mammalian sGC $\alpha 1/\beta 1$ (*26*). Oxygen, CO, and NO inhibit the activity of Fe(II)-unligated Gyc-88E(1−597) by 3.2-, 2.9-, and 2-fold, respectively (Figure 3B). This type of regulation is quite distinct from the mechanism of regulation of the NO-sensitive sGC, which is insensitive to O_2 and activated from the basal state about 200-fold by NO and 4-fold by CO (*25*).

Affinity of Gyc-88E(1−597) for O_2. Finally, the affinity of Gyc-88E(1−597) for oxygen was determined by measuring the specific activity at different O_2 concentrations (Figure 4A). The inhibition of Gyc-88E(1−597) could be fit to either hyperbolic mixed-type inhibition or a model of partial noncompetitive inhibition in which the inhibition is reversible, the enzyme−substrate−inhibitor complex is productive, and the V_{max} is changed with the inhibitor. We chose the hyperbolic mixed-type model because the K_m values with and without O_2 were different, although the change was small (*22*). After fitting of the data to the equation for hyperbolic mixed-type inhibition (*22*), β and αK_i were found to be 0.26 ± 0.076 and 41 ± 19 μM, respectively. To calculate K_i, α was determined by measuring the K_m for GTP-Mg^{2+} in air (273 μM O_2) and deoxygenated buffer (Figure 4B). The K_m was 0.66 ± 0.15 mM in the presence of air and 0.82 ± 0.15 mM in the absence of air. The K_i was thus calculated to be 51 ± 28 μM. Inhibition by oxygen appears to occur more via a change in V_{max} than a change in K_m. Moreover, the micromolar K_i falls within the range of reasonable oxygen concentrations that *Drosophila* would experience.

DISCUSSION

NO is highly toxic and reactive with O_2. These properties require receptors for NO in cellular signaling to be highly sensitive and selective. sGC meets these demands but does so using a ferrous protoporphyrin IX heme with histidine ligation as the receptor for NO. Despite having a heme cofactor identical to that of the globins, sGC has no measurable affinity for O_2 (*25*). This ligand discrimination against O_2 is critical for NO signaling, and over the last 3 years a molecular explanation has emerged for this ligand exclusion. As mentioned above, sGC is part of the H−NOX family where the presence of a distal pocket tyrosine is crucial for the formation of stable O_2 complexes. The absence of such a H-bonding distal pocket residue leads to no or little O_2 binding.

With the apparent basis for ligand discrimination against O_2, we searched genomes for sGCs that would potentially form a stable O_2 complex and, therefore, might also be regulated by O_2. It should be stated that all ferrous hemoproteins that bind O_2 also form complexes with NO and CO, so biological regulation will have to involve further studies to determine in vivo function. We used the sequence alignments (Figure 1A) and homology models to predict that the atypical *Drosophila* sGCs would bind O_2, but the only evidence supporting this prediction has been assays with COS-7 cell lysates (*12*). Through the cloning, purification, and subsequent characterization of Gyc-88E(1−597), we were able to show definitively that it is an oxygen-binding heme protein with guanylate cyclase activity. Unlike typical sGC, oxygen binds to Gyc-88E, forming a 6-coordinate complex that inhibits the inherent cyclase activity. The ~3-fold level of inhibition is, however, similar to the 4-fold level of activation by CO and the ~4-fold change between the tonic and fully activated states of mammalian sGC $\alpha 1/\beta 1$ (*27*). Similar to other proteins that function as O_2 binders, such as the globins (*23*), Gyc-88E also binds NO and CO, forming 6-coordinate complexes that inhibit cyclase activity 2−3-fold. In contrast, NO forms a 5-coordinate complex and CO forms a 6-coordinate complex with mammalian sGC, activating it several hundred-fold above basal and 4-fold, respectively (*3*).

Another property that makes Gyc-88E unique from classical sGC, an obligate heterodimer (*3*), is that it is active as a homodimer. This is consistent with the prediction that the *Drosophila* atypical sGCs can form three active dimers: Gyc-88E homodimer, Gyc-88E/Gyc-89Da, and Gyc-88E/Gyc-89Db (*11*, *12*, *17*, *18*). The physiologically relevant dimer(s) remains to be determined. It is possible that the dimer composition varies depending on the cell type and life stage and that each has unique biochemical properties that are exploited to achieve specific biological functions. In vivo studies, presently under way, will undoubtedly help address these questions.

Our findings show that Gyc-88E binds and is inhibited by O_2, the very ligand that classical sGC has evolved not to bind. This unique characteristic of Gyc-88E, combined with its expression in peripheral neurons that innervate the trachea in embryos and larvae (*12*, *15*), supports a function as an oxygen sensor. Importantly, the K_i of O_2 falls in the range of physiologically reasonable oxygen concentrations within the organism. Moreover, the significant change we observe in cGMP production in response to oxygen is of a magnitude capable of mediating important biological processes, as cGMP is a second messenger that amplifies signals by orders of magnitude through downstream signaling cascades. For example, a 2−3-fold decrease in cGMP levels can cause significant increases in tension within bovine intrapulmonary arteries and veins (*28*). Additionally, a 2-fold increase in cGMP levels stimulates fluid secretion substantially from the Malpighian tubules in *Drosophila* (*29*, *30*).

Although saturating amounts of NO and CO inhibit Gyc-88E activity like oxygen in vitro, the atypical sGCs may be regulated by these ligands differently in vivo. Indeed, the concentrations of NO and CO in cells expressing Gyc-88E may be too low to compete with O_2 for binding, similar to the globins that function with oxygen in the presence of low concentrations of NO and CO. *Drosophila* does have a nitric oxide synthase (*31*), heme oxygenase (*32*), and NO-sensitive sGC (*1*, *2*), but it is not known whether they are temporally and spatially coexpressed with Gyc-88E. A model for hypoxia sensing in *Drosophila* larvae and embryos was previously proposed to be mediated by a pathway involving NO, sGC, and PKG (*33*). However, the sGC isoform involved and the protein(s) responsible for sensing the change in O_2 levels have not been identified. Further studies could reveal that Gyc-88E plays an important role in this oxygen-sensing pathway.

All detailed mechanistic studies with purified sGCs to date have been on the NO-regulated enzymes that do not bind oxygen (*3*, *13*, *34*). Despite years of research, questions concerning mechanisms of activation remain unanswered. Many insights can be gained from comparing these NO-specific sGCs to the new class of atypical sGCs, but no purified protein model of an atypical sGC has been available until now. The ligand-induced effect on activity is exactly the opposite when the classical sGCs are compared to the atypical one described here. NO and CO (albeit weakly) activate the classical sGCs while those ligands and O_2 inhibit Gyc-88E, suggesting significant differences in the way signals from ligand binding to the H−NOX domain are communicated to the catalytic domain of classical versus atypical sGCs. Further biochemical studies with the *Drosophila* atypical sGCs will contribute to the understanding of how both classes of sGCs are regulated.

Not only are the biochemical properties of Gyc-88E unique in the cyclase family, but they also raise interesting biological questions concerning its possible function and regulation in vivo. The combination of an O_2-sensing H−NOX domain with a cyclase catalytic domain may have been nature's way of making a new sensor for oxygen that causes a more direct and immediate response than transcription-mediated sensors such as the HIF-1 transcription factor. Indeed, there is evidence that *C. elegans* may have an O_2 sensor, which could serve to induce social and feeding behaviors or avoid toxic O_2 concentrations on second to minute time scales (*10*, *35*). Analogously, *Drosophila* larvae have PKG-dependent foraging behaviors that are affected by changing oxygen levels (*33*). Moreover, there is evidence that insects such as *D. melanogaster* need a fast-acting oxygen sensor to control the amount of O_2 that enters their trachea (*36*). Since the atypical fly sGCs are expressed in neurons that innervate the trachea (*15*), they could be functioning to control the opening and closing of spiracles. Further characterization can help to elucidate mechanisms of oxygen sensing that may relate to feeding, breathing, or chemotactic behaviors.

ACKNOWLEDGMENT

We thank Dr. Svetlana Dzitoyeva (University of Illinois) for the *Drosophila* embryonic cDNA library and are grateful to the Marletta Lab for stimulating discussions; in particular, we thank Emily R. Derbyshire for discussions about sGC and Jacquin C. Niles for discussions about the biological implications of our results.

REFERENCES

1. Liu, W., Yoon, J., Burg, M., Chen, L., and Pak, W. L. (1995) Molecular characterization of two *Drosophila* guanylate cyclases expressed in the nervous system, *J. Biol. Chem. 270*, 12418−12427.
2. Shah, S., and Hyde, D. R. (1995) Two *Drosophila* genes that encode the alpha and beta subunits of the brain soluble guanylyl cyclase, *J. Biol. Chem. 270*, 15368−15376.
3. Denninger, J. W., and Marletta, M. A. (1999) Guanylate cyclase and the NO/cGMP signaling pathway, *Biochim. Biophys. Acta. 1411*, 334−350.
4. Boon, E. M., and Marletta, M. A. (2005) Ligand discrimination in soluble guanylate cyclase and the H-NOX family of heme sensor proteins, *Curr. Opin. Chem. Biol. 9*, 441−446.
5. Boon, E. M., Huang, S. H., and Marletta, M. A. (2005) A molecular basis for NO selectivity in soluble guanylate cyclase, *Nat. Chem. Biol. 1*, 53−59.
6. Karow, D. S., Pan, D., Tran, R., Pellicena, P., Presley, A., Mathies, R. A., and Marletta, M. A. (2004) Spectroscopic characterization of the soluble guanylate cyclase-like heme domains from *Vibrio cholerae* and *Thermoanaerobacter tengcongensis*, *Biochemistry 43*, 10203−10211.
7. Nioche, P., Berka, V., Vipond, J., Minton, N., Tsai, A.-L., and Raman, C. S. (2004) Femtomolar sensitivity of a NO sensor from *Clostridium botulinum*, *Science 306*, 1550−1553.
8. Pellicena, P., Karow, D. S., Boon, E. M., Marletta, M. A., and Kuriyan, J. (2004) Crystal structure of an oxygen-binding heme domain related to soluble guanylate cyclases, *Proc. Natl. Acad. Sci. U.S.A. 101*, 12854−12859.
9. Boon, E. M., and Marletta, M. A. (2005) Ligand specificity of H-NOX domains: from sGC to bacterial NO sensors, *J. Inorg. Biochem. 99*, 892−902.
10. Gray, J. M., Karow, D. S., Lu, H., Chang, A. J., Chang, J. S., Ellis, R. E., Marletta, M. A., and Bargmann, C. I. (2004) Oxygen sensation and social feeding mediated by a *C. elegans* guanylate cyclase homologue, *Nature 430*, 317−322.
11. Morton, D. B. (2004) Invertebrates yield a plethora of atypical guanylyl cyclases, *Mol. Neurobiol. 29*, 97−116.
12. Morton, D. B. (2004) Atypical soluble guanylyl cyclases in *Drosophila* can function as molecular oxygen sensors, *J. Biol. Chem. 279*, 50651−50653.
13. Cary, S. P. L., Winger, J. A., Derbyshire, E. R., and Marletta, M. A. (2006) Nitric oxide signaling: no longer simply on or off, *Trends Biochem. Sci. 31*, 231−239.
14. Iyer, L. M., Anantharaman, V., and Aravind, L. (2003) Ancient conserved domains shared by animal soluble guanylyl cyclases and bacterial signaling proteins, *BMC Genomics 4*, 5.
15. Morton, D. B., Langlais, K. K., Stewart, J. A., and Vermehren, A. (2005) Comparison of the properties of the five soluble guanylyl cyclase subunits in *Drosophila melanogaster*, *J. Insect Sci. 5*, No. 12.
16. Riedl, C. A. L., Neal, S. J., Robichon, A., Westwood, J. T., and Sokolowski, M. B. (2005) *Drosophila* soluble guanylyl cyclase

mutants exhibit increased foraging locomotion: behavioral and genomic investigations, *Behav. Genet. 35*, 231−244.
17. Liu, Y., Ruoho, A. E., Rao, V. D., and Hurley, J. H. (1997) Catalytic mechanism of the adenylyl and guanylyl cyclases: Modeling and mutational analysis, *Proc. Natl. Acad. Sci. U.S.A. 94*, 13414−13419.
18. Vermehren, A., Langlais, K. K., and Morton, D. B. (2006) Oxygen-sensitive guanylyl cyclases in insects and their potential roles in oxygen detection and in feeding behaviors, *J. Insect Physiol. 52*, 340−348.
19. Cavener, D. R. (1987) Comparison of the consensus sequence flanking translational start sites in *Drosophila* and vertebrates, *Nucleic Acids Res. 15*, 1353−1361.
20. Ausubel, F. M., et al. (2007) *Current Protocols in Molecular Biology*, John Wiley & Sons, Inc., New York.
21. Dean, J. A. (1999) *Lange's Handbook of Chemistry*, 15th ed., McGraw-Hill, New York.
22. Segel, I. H. (1975) *Enzyme Kinetics, Behavior and Analysis of Rapid Equilibrium and Steady-State Enzyme Systems*, John Wiley & Sons, Inc., New York.
23. Antonini, E., and Brunori, M. (1971) *Hemoglobin and Myoglobin in Their Reactions with Ligands*, North-Holland Publishing Co., Amsterdam.
24. Boon, E. M., Davis, J. H., Tran, R., Karow, D. S., Huang, S. H., Pan, D., Miazgowicz, M. M., Mathies, R. A., and Marletta, M. A. (2006) Nitric oxide binding to prokaryotic homologs of the soluble guanylate cyclase β1 H-NOX domain, *J. Biol. Chem. 281*, 21892−21902.
25. Stone, J. R., and Marletta, M. A. (1994) Soluble guanylate cyclase from bovine lung: activation with nitric oxide and carbon monoxide and spectral characterization of the ferrous and ferric states, *Biochemistry 33*, 5636−5640.
26. Derbyshire, E. R., Tran, R., Mathies, R. A., and Marletta, M. A. (2005) Characterization of nitrosoalkane binding and activation of soluble guanylate cyclase, *Biochemistry 44*, 16257−16265.
27. Cary, S. P. L., Winger, J. A., and Marletta, M. A. (2005) Tonic and acute nitric oxide signaling through soluble guanylate cyclase is mediated by nonheme nitric oxide, ATP, and GTP, *Proc. Natl. Acad. Sci. U.S.A. 102*, 13064−13069.
28. Ignarro, L. J., Byrns, R. E., and Wood, K. S. (1987) Endothelium-dependent modulation of cGMP levels and intrinsic smooth muscle tone in isolated bovine intrapulmonary artery and vein, *Circ. Res. 60*, 82−92.
29. Davies, S. A., Huesmann, G. R., Maddrell, S. H., O'Donnell, M. J., Skaer, N. J., Dow, J. A., and Tublitz, N. J. (1995) CAP2b, a cardioacceleratory peptide, is present in *Drosophila* and stimulates tubule fluid secretion via cGMP, *Am. J. Physiol.: Regul., Integr. Comp. Physiol. 269*, R1321−1326.
30. Dow, J. A., Maddrell, S. H., Davies, S. A., Skaer, N. J., and Kaiser, K. (1994) A novel role for the nitric oxide-cGMP signaling pathway: the control of epithelial function in *Drosophila*, *Am. J. Physiol.: Regul., Integr. Comp. Physiol. 266*, R1716−1719.
31. Regulski, M., Stasiv, Y., Tully, T., and Enikolopov, G. (2004) Essential function of nitric oxide synthase in *Drosophila*, *Curr. Biol. 14*, R881−882.
32. Zhang, X., Sato, M., Sasahara, M., Migita, C. T., and Yoshida, T. (2004) Unique features of recombinant heme oxygenase of *Drosophila melanogaster* compared with those of other heme oxygenases studied, *Eur. J. Biochem. 271*, 1713−1724.
33. Wingrove, J. A., and O'Farrell, P. H. (1999) Nitric oxide contributes to behavioral, cellular, and developmental responses to low oxygen in *Drosophila*, *Cell 98*, 105−114.
34. Poulos, T. L. (2006) Soluble guanylate cyclase, *Curr. Opin. Struct. Biol. 16*, 736−743.
35. Rogers, C., Persson, A., Cheung, B., and de Bono, M. (2006) Behavioral Motifs and Neural Pathways Coordinating O_2 Responses and Aggregation in *C. elegans*, *Curr. Biol. 16*, 649−659.
36. Hetz, S. K., and Bradley, T. J. (2005) Insects breathe discontinuously to avoid oxygen toxicity, *Nature 433*, 516−519.
37. Thompson, J. D., Higgins, D. G., and Gibson, T. J. (1994) CLUSTAL W: improving the sensitivity of progressive multiple sequence alignment through sequence weighting, position-specific gap penalties and weight matrix choice, *Nucleic Acids Res. 22*, 4673−4680.

BI701771R